

## Characterization of a novel fungal immunomodulatory protein, FIP-SJ75 shuffled from *Ganoderma lucidum*, *Flammulina velutipes* and *Volvariella volvacea*

Ke-Di Shao, Pei-Wen Mao, Qi-Zhang Li, Liu-Ding-Ji Li, Yu-liang Wang & Xuan-Wei Zhou

To cite this article: Ke-Di Shao, Pei-Wen Mao, Qi-Zhang Li, Liu-Ding-Ji Li, Yu-liang Wang & Xuan-Wei Zhou (2019) Characterization of a novel fungal immunomodulatory protein, FIP-SJ75 shuffled from *Ganoderma lucidum*, *Flammulina velutipes* and *Volvariella volvacea*, Food and Agricultural Immunology, 30:1, 1253-1270, DOI: [10.1080/09540105.2019.1686467](https://doi.org/10.1080/09540105.2019.1686467)

To link to this article: <https://doi.org/10.1080/09540105.2019.1686467>



© 2019 The Author(s). Published by Informa UK Limited, trading as Taylor & Francis Group



View supplementary material [↗](#)



Published online: 12 Nov 2019.



Submit your article to this journal [↗](#)



Article views: 927



View related articles [↗](#)




View Crossmark data [↗](#)



Citing articles: 6 View citing articles [↗](#)

## Characterization of a novel fungal immunomodulatory protein, FIP-SJ75 shuffled from *Ganoderma lucidum*, *Flammulina velutipes* and *Volvariella volvacea*

Ke-Di Shao, Pei-Wen Mao, Qi-Zhang Li, Liu-Ding-Ji Li, Yu-liang Wang and Xuan-Wei Zhou 

Key Laboratory of Urban Agriculture (South) Ministry of Agriculture, and Engineering Research Center of Cell & Therapeutic Antibody, Ministry of Education, School of Agriculture and Biology, Shanghai Jiao Tong University, Shanghai, People's Republic of China

### ABSTRACT

*FIP-SJ75*, a novel fungal immunomodulatory protein gene, was shuffled from the genes of three different mushroom species: *Ganoderma lucidum*, *Flammulina velutipes*, and *Volvariella volvacea*. Based on the expression of *FIP-SJ75* gene in *Escherichia coli*, recombinant FIP-SJ75 (rFIP-SJ75) was routinely confirmed, consisting of 115 amino acids, and six peptides were identified by LC/Q-TOF MS with a coverage rate of 84.3%. Bioactivity assay *in vitro* indicated that rFIP-SJ75 promoted the proliferation of RAW264.7 cells at a range of 1–8 µg/mL, and significantly activated RAW264.7 cells in a dose-dependent manner. Real-time PCR revealed rFIP-SJ75 obviously promoted pro-inflammatory genes (*TNF-α* and *IL-6*), but reduced the expression of anti-inflammatory genes (*IL-10* and *TGF-β1*) at the transcriptional level. These data implied that rFIP-SJ75 possessed immunomodulatory activity in macrophages by promoting macrophage M1 polarization and initiating pro-inflammatory responses, which could lay the foundation for rFIP-SJ75 to become a stable immunomodulator resource for further research and potential applications.

### ARTICLE HISTORY


Received 11 October 2019  
Accepted 23 October 2019


### KEYWORDS

Fungal immunomodulatory protein; expression; mouse macrophage RAW264.7 cells; macrophage activation; inflammation

## 1. Introduction

Fungal immunomodulatory protein (FIP) is a species of small molecular weight protein derived from some medicinal and edible mushrooms, which shares considerable structural and functional similarity (Li, Wang, & Zhou, 2011; Wang et al., 2012). The structure of FIPs is similar to phytohemagglutinin and immunoglobulin, and the wild-type FIPs exist as homodimers (Williams & Barclay, 1988; Xu et al., 2016). The first FIP, designated as FIP-glu (LZ-8), was isolated from *Ganoderma lucidum* (Kino et al., 1989). Until now,

**CONTACT** Xuan-Wei Zhou  xuanweizhou163.com; Yu-Liang Wang  wangyuliangsjtu.edu.cn  Key Laboratory of Urban Agriculture (South) Ministry of Agriculture, and Engineering Research Center of Cell & Therapeutic Antibody, Ministry of Education, School of Agriculture and Biology, Shanghai Jiao Tong University, No. 311# Agriculture and Biology New Building, 800 Dongchuan Road, Shanghai, People's Republic of China

 Supplemental data for this article can be accessed <https://doi.org/10.1080/09540105.2019.1686467>

© 2019 The Author(s). Published by Informa UK Limited, trading as Taylor & Francis Group

This is an Open Access article distributed under the terms of the Creative Commons Attribution-NonCommercial-NoDerivatives License (<http://creativecommons.org/licenses/by-nc-nd/4.0/>), which permits non-commercial re-use, distribution, and reproduction in any medium, provided the original work is properly cited, and is not altered, transformed, or built upon in any way.

FIPs have been isolated and identified from several fungi, such as *Flammulina velutipes* (FIP-fve) (Ko, Hsu, Lin, Kao, & Lin, 1995), *Volvariella volvacea* (FIP-vvo) (Hsu, Hsu CI, Kao, & Lin, 1997), *Auricularia polytricha* (FIP-app) (Sheu, Chien, Chien, Chen, & Chin, 2004), *Ganoderma microsporum* (FIP-gmi) (Wu et al., 2007), *Ganoderma sinense* (FIP-gsi) (Zhou, Xie, Hong, & Li, 2009), *Poria cocos* (FIP-pcp) (Chang, Yeh, & Sheu, 2009), *Trametes versicolor* (FIP-tvc) (Li, Wen, Liu, Zhou, & Chen, 2012), *Nectria haematococca* (FIP-nha) (Bastiaan-Net et al., 2013), *Ganoderma lucidum* (LZ-9) (Bastiaan-Net et al., 2013), *Postia placenta* (FIP-ppl) (Li, Shi, Ding, Nie, & Tang, 2015), *Ganoderma atrum* (FIP-gat) (Xu et al., 2016), *Chroogomphus rutilus* (FIP-cru) (Lin et al., 2016), *Dichomitus squalens* (FIP-dsq2) (Li et al., 2017), *Ganoderma applanatum* (FIP-gap) (Zhou et al., 2018), and *Lentinus tigrinus* (FIP-lti) (Gao et al., 2019). A protein family called FIPs was composed of these proteins (Li et al., 2011). Analysis of the previous literature, in addition to traditional protein purification, we found that FIPs can be made by homologous cloning, directed revolutionary and genome mining methods. The source of FIPs is not confined to mushrooms, but also other filamentous fungi.

*FIP-SJ75* is a recombinant DNA sequence generated shuffled from *FIP-glu* (Genbank accession no. M58032.1), *FIP-fve* (Genbank accession no. GU388420.1) and *FIP-vvo* (Hsu et al., 1997), which are isolated from *G. lucidum* (ACCC 50044), *G. velutipes* (ACCC 50007) and *V. volvacea* (ACCC 50425), respectively. FIP-SJ75 is composed of 115 amino acids and has an agglutination effect on mouse erythrocytes when the concentration is greater than 1.56  $\mu\text{g}/\text{mL}$  (Wang et al., 2013). FIPs have several biological activities *in vitro* (Li et al., 2015). A large body of literature has documented that FIPs exert many important preventive and therapeutic functions, for instance, hemagglutination, anti-tumor, anti-allergy, anti-virus, immune-cell proliferation and regulation of cytokine expression (Cong et al., 2014; Li et al., 2011; Li, Bu, Li, & Wu, 2019; Zhou et al., 2018). Immune organs and immune cells constitute the immune system and exert immune function (Leiro, Castro, Arranz, & Lamas, 2007). Macrophages play a vital role in the immune response (Davies, Jenkins, Allen, & Taylor, 2013). RAW264.7 is a mouse mononuclear macrophage that exerts immunity through phagocytosis, stimulation of antigens, and production of cytokines (Sica, Erreni, Allavena, & Porta, 2015; Wang et al., 2019). Therefore, it can be used to simulate the immunomodulation of macrophages *in vivo* and for immunological research (Lee & Lim, 2008). Macrophages can be activated by Toll-like receptor (TLR) to release a series of pro-inflammatory (TNF- $\alpha$ , IL-6, IL-1, etc.) or anti-inflammatory (IL-10, TGF- $\beta$ 1, etc.) mediators (Hug, Mohajeri, & La Fata, 2018; Nonnenmacher & Hiller, 2018). Furthermore, the TLR-dependent activation can be regulated by FIPs. For example, FIP-pcp is capable of activating murine macrophages via cytokine production and NF- $\kappa$ B-dependent regulation (Chang et al., 2009). FIP-glu (LZ-8) exerts immunomodulatory activity by modulating pro-inflammatory and anti-inflammatory mediators to induce M1 polarization in macrophages (Li, Chang, He, Chen, & Zhou, 2019).

In this study, four FIPs genes including *FIP-SJ75*, *FIP-glu*, *FIP-fve* and *FIP-vvo* were routinely expressed in *E. coli*, and the recombinant proteins were confirmed by SDS-PAGE and Western Blot. Purified recombinant FIP-SJ75, a new FIP, was subjected to protein identification by liquid chromatography coupled with quadrupole time-of-flight mass spectrometry (LC/Q-TOF MS). The rFIPs were furtherly used for investigating their biological activities on inducing macrophage activation and the production of pro-inflammatory and anti-inflammatory mediators. Base on bioinformatics analysis of the

FIPs, we analyzed the signal transduction pathways of its immune regulation coupled with the data of the real-time quantitative polymerase chain reaction (RT-qPCR). All of those results implied that rFIP-SJ75 had potential as a regulator of immune responses and was of great importance in the prevention and treatment of human immunosuppression.

## 2. Materials and methods

### 2.1. Materials

*FIP-SJ75*, *FIP-glu*, *FIP-fve*, and *FIP-vvo* genes and pCold TF expression vector were preserved by our laboratory. The pMD18-T vector was purchased from Takara Biotechnology Co., Ltd. (Dalian, China). The *E. coli* Rosetta (DE3) was purchased from Sangon Biotech Co., Ltd. (Shanghai, China).

### 2.2. Methods

#### 2.2.1. Sequence alignment and structure modelling

The peptide sequences of FIP-SJ75 were deduced from the nucleotide sequences of *FIP-SJ75* genes. The isoelectric points (pI) and theoretical molecular weights (MW) were calculated using ExPASy ProtParam. The amino acid sequences of FIP-SJ75 and the reported 15 FIPs were aligned by using Lasergene 7.1 software (DNASTAR, Inc., USA). The secondary structure of FIP-SJ75 and the other three parental FIPs was predicted by the Sopma programme. The structure modelling was carried out by the MODELLER 9.18 software. The crystal structures of FIP-glu (3F3H) and FIP-fve (1OSY) were served as templates.

#### 2.2.2. Hydrophobicity and hydrophilicity

The Kyte-Doolittle hydropathy index of FIP-SJ75 and other three parental proteins was analyzed by BioEdit 7.2.5 software. The window size was set to 9, and the hydrophilic/hydrophobic range was from  $-2.8$  to  $+2.8$ .

#### 2.2.3. Phylogenetic tree construction

The phylogenetic tree was constructed by the MEGA 7 software (Felsenstein, 1985). The statistical confidence of the phylogenetic relationship was repeated 1000 times by the bootstrap test.

#### 2.2.4. Construction of expression vector

The *FIP-SJ75* gene had been cloned into the pMD18-T vector previously. Two primers, FIP-SJ75-F (SacI: 5'-AAGGTAGGCATATGGAGCTCATGAGCACC-3') and FIP-SJ75-R (XbaI: 5'-ATTACCTATCTAGACTGCAGCTATTTTCAGTTC-3') were designed using PRIMER (version 6). After gene amplification using PCR, the *FIP-SJ75* gene and plasmid pCold TF were digested with SacI and XbaI. Then digested genes were ligated into linearized vector pCold TF with T4 DNA ligase (Sangon, Shanghai, China) to construct the recombinant plasmid pCold TF-FIP-SJ75. Using the same method to clone the parental FIPs, FIP-glu (GeneBank: ACD44335.1), FIP-fve (GenBank: ADB24832.1), and FIP-vvo (Hsu et al., 1997), which were used as controls, and the following primers

were used: FIP-glu-F (SacI: 5'-AAGGTAGGCATATGGAGCTCATGTCTGAT-3'), FIP-glu-R (XbaI: 5'-ATTACCTATCTAGACTGCAGCTAGTTCCATTGA-3'), FIP-fve-F (SacI: 5'-AAGGTAGGCATATGGAGCTCATGTCCGCC-3'), FIP-fve-R (XbaI: 5'-ATTACCTATCTAGACTGCAGCTATTACTTCTT-3'), FIP-vvo-F (SacI: 5'-AAGGTAGGCATATGGAGCTCATGAGCACT-3'), FIP-vvo-R (XbaI: 5'-ATTACCTATCTAGACTGCAGCTACTTCCATTG-3'). The ligated products were transformed into *E. coli* Rosetta (DE3) competent cells (Sangon Bio Inc., Shanghai, China).

### 2.2.5. Protein expression

The positive transformants were screened on Luria-Bertani (LB) agar solid plates containing 100 µg/mL ampicillin and verified by colony PCR and sequencing. The positive monoclonal strain was cultured at 37 °C until OD<sub>600</sub> was 0.4–0.5. Isopropyl-β-D-thiogalactoside (IPTG) was added to a final concentration of 1 mM, and the culture was incubated for 5 h at 16 °C. The cells were harvested by centrifugation at 4000 × g for 10 min at 4 °C. Then it was resuspended in 10 µL of 5 × SDS-PAGE loading buffer and boiled for 5 min at 100 °C. After centrifugation, the expression products were analyzed by 10% SDS-PAGE.

### 2.2.6. Induction time optimization and Western blot assays

To determine the optimal time for inducing expression rFIP-SJ75 in *E. coli* Rosetta (DE3) cells, five different time gradients (0, 4, 8, 12, and 24 h) were selected for induction. The crude proteins were dissolved in lysis buffer (50 mM NaH<sub>2</sub>PO<sub>4</sub>, 300 mM NaCl, 10 mM imidazole, pH 8.0) and mixed with 5 × loading buffer. After all samples were boiled for 5 min, the expression product was analyzed by 10% SDS-PAGE and visualized by staining with Coomassie Brilliant Blue R-250. The protein samples resolved in gel were transferred to a 0.2 µm polyvinylidene fluoride membranes (PVDF) in a Bio-rad Trans-Blot system for Western blot. After blocking with TBST containing 5% skim dry milk and washing three times with TBST, the PVDF membrane was immune-detected with the anti-His monoclonal antibody produced in mouse (Sangon Bio Inc., China, 1:10,000 diluted) as the primary antibody. And the HRP-conjugated anti-mouse IgG produced in goat (Sangon Bio Inc., 1:5000 diluted) was used as the secondary antibody. After covering with the TMB reagent (Beyotime, China), the PVDF membrane was incubated in dark conditions for 5 min until colour development.

### 2.2.7. Purification of rFIPs

Purification of recombinant rFIPs was carried out with a nickel-nitrilotriacetic acid (Ni-NTA) agarose resin column (Takara Bio Inc., Dalian, China). The rFIPs after purification, dialysis, and lyophilization were dissolved with PBS and the purity was analyzed by SDS-PAGE. The concentration of rFIPs was measured by Bradford Protein Assay Kit (Sangon Bio Inc., Shanghai, China). After that, proteins were digested with the help of a Thrombin kit (Merck, Darmstadt, Germany) at 4 °C for 24 h to remove His-tag and Trigger Factor and were analyzed by SDS-PAGE.

### 2.2.8. Identification of rFIP-SJ75 and determination of lipopolysaccharide (LPS) concentration

The gel slice was excised from the polyacrylamide gel containing the target protein and was destained. After digestion with trypsin at 37 °C overnight, the digested rFIP-SJ75

was subjected to protein identification by LC/Q-TOF MS (Applied Biosystems, Foster City, CA, USA), which was performed at the Instrumental Analysis Center of SJTU. The detected peptide masses matched the rFIP-SJ75 peptide sequence. LPS levels in the purified rFIPs were measured using an ELISA kit (Cloude-Clone Corp., Houston, TX, USA) to calculate the content of LPS present in culture media when different doses of rFIPs were applied in the subsequent cell assays.

### **2.2.9. Cell culture**

Macrophage RAW264.7 cells were purchased from the Cell Bank of the Chinese Academy of Sciences (Shanghai, China). Cells were cultivated in DMEM (HyClone, GE) supplemented with 100 U/mL penicillin, 100 mg/mL streptomycin (Gibco, Rockville, MD), and 10% fetal bovine serum (HyClone, GE) and incubated at 37 °C in a 5% CO<sub>2</sub> incubator. RAW264.7 cells were digested with 0.25% trypsin containing 0.04% EDTA.

### **2.2.10. Cytotoxicity assay on RAW264.7**

RAW264.7 cell suspension ( $2.5 \times 10^5$  cell/mL) was inoculated into a 96-well microplate at 100  $\mu$ L per well and incubated for 24 h. Thereafter, serially diluted rFIP-SJ75, rFIP-glu, rFIP-fve, and rFIP-vvo were added into 96-well microplate at 100  $\mu$ L per well (final concentrations of 1, 2, 4, 8, 16, and 32  $\mu$ g/mL, respectively). PBS, lipopolysaccharide (LPS, 1  $\mu$ g/mL), and Concanavalin A (ConA, 5  $\mu$ g/ml) were used as controls. After incubating for 24 h, RAW264.7 cell viabilities were assessed by CCK assay. Absorbance values were measured at 450 nm using a microplate reader (BIO-TEK®), and the viability was expressed as a percentage relative to the control group.

### **2.2.11. Phagocytosis assay**

The phagocytosis assay was performed by a neutral red uptake assay (Xiong et al., 2018). RAW264.7 cells were suspended to  $2.5 \times 10^5$  cell/mL in 96-well microplate and incubated for 24 h. Subsequently, serially diluted rFIP-SJ75, rFIP-glu, rFIP-fve, and rFIP-vvo were added into 96-well microplate at 100  $\mu$ L per well (final concentrations of 1, 2, 4, 8, and 16  $\mu$ g/mL, respectively). Meanwhile, a final concentration of 8  $\mu$ g/mL rFIPs treated RAW264.7 cells to verify the effect of different rFIPs on the phagocytosis. PBS and ConA (5  $\mu$ g/mL) were used as controls. After incubating 24 h, the supernatant was discarded and added 100  $\mu$ L neutral red staining solution into per well. The supernatant was discarded again after incubating for 30 min. The cells were washed with PBS for three times, and 200  $\mu$ L cell lysis buffer (ethanol:acetic acid = 1:1 [volume]) were added to per well. Absorbance values were measured at 540 nm using a microplate reader (BIO-TEK®). Finally, phagocytosis was indicated by the optical density (OD) value.

### **2.2.12. Inflammatory genes induction of rFIP-SJ75**

To access the immunomodulatory activity of rFIP-SJ75, different expressions of pro-inflammatory and anti-inflammatory genes were analyzed by quantitative real-time polymerase chain reaction (RT-qPCR). Murine macrophage RAW264.7 cells were adjusted to  $2.5 \times 10^5$  cell/mL in 12-well microplate. After 6 h of culture in DMEM medium containing 8  $\mu$ g/mL of rFIP-SJ75, rFIP-glu, rFIP-fve, and rFIP-vvo, RAW264.7 cells were harvested. Total RNA was extracted using the RNAPrep pure Cell/Bacteria Kit (Tiangen, Beijing, China). cDNA was synthesized from RNA using HiScript RT SuperMix (Vazyme,

Nanjing, China) according to the manufacturer's protocol. RT-qPCR was performed using the SYBR qPCR Master Mix (Vazyme, Nanjing, China). The RT-qPCR primer sequences were listed in Table 1. All reactions were performed in three biological replicates, and the Ct value was normalized to  $\beta$ -actin. The relative expression of inflammatory genes was calculated using the  $2^{-\Delta\Delta Ct}$  method.

### 2.3. Statistical analysis

Graphs and statistical analysis were prepared using GraphPad Prism 5 software (GraphPad Software Inc., La Jolla, CA, USA). Data were presented as the mean  $\pm$  SD. Statistical analysis was performed using one-way analysis of variance (ANOVA). Significance was indicated as ns,  $p > 0.05$ ; \* or #,  $p < 0.05$ ; \*\* or ##,  $p < 0.01$ ; \*\*\* or ###,  $p < 0.0001$ .

## 3. Results

### 3.1. Bioinformatics analysis of FIP-SJ75

A new rFIP, designated as FIP-SJ75, was obtained from three different mushroom species (*G. lucidum*, *F. velutipes*, and *V. volvacea*) by DNA shuffling technology. Sequencing data showed that *FIP-SJ75* comprised 345-bp. Meanwhile, peptide sequences contained 115 amino acids with a molecular weight of 12,952 Da and a pI of 7.68. Amino acid sequence alignment showed that FIP-SJ75 had high homology with other FIPs (Percent identity: 59.8% with FIP-glu and FIP-gts, 62.8% with FIP-cru1, 66.3% with FIP-dsq2, 49.1% with FIP-fve, 63.8% with FIP-gap1, 58.5% with FIP-gap2, 64.0% with FIP-gat, 58.8% with FIP-gja, 67.4% with FIP-gmi, 69.7% with LZ-9, 64.5% with FIP-nha, 58.4% with FIP-sch2, 94.7% with FIP-vvo, and 61.7% with FIP-ppl, respectively; Figure 1(a)). Predicted secondary structure of FIP-SJ75, FIP-glu, and FIP-vvo contained two  $\alpha$ -helix and seven extended-strands, whereas FIP-fve contained two  $\alpha$ -helix and six extended-strands (Figure 1(b)). A homology model of the 3D structure of FIP-SJ75 was constructed using the crystal structures of FIP-glu and FIP-fve as templates (Figure 1(c)). Except for the N-terminal  $\alpha$ -helix, loopDE, and loopFG regions, FIP-SJ75 can be highly coincident with most of the other three parental proteins.

The hydrophobicity profile showed that the N-terminal of four FIPs was hydrophobic, while the C-terminal was hydrophilic. The values of hydrophobicity and hydrophilicity were roughly similar between the four FIPs, but there were still some differences between certain regions (Figure 2(a)).

The phylogenetic tree showed that FIP-glu (LZ-8), FIP-gts, FIP-gja, FIP-gat, LZ-9, FIP-gmi, FIP-gap2, FIP-cru1, FIP-gap1, FIP-fve, and FIP-nha clustered into one main lineage.

**Table 1.** Primers for qPCR.

Gene	Forward Primer	Reverse Primer
TNF- $\alpha$	TTCTATGGCCCAGACCCTCA	ACAAGGTACAACCCATCGGC
IL-6	CATGTTCTCTGGGAAATCGTGG	AACGCACTAGGTTTGCCGAGTA
IL-10	CAGTACAGCCGGGAAGACAA	AGGAGTCGGTTAGCAGTATGT
TGF- $\beta$ 1	ACAGCACCAATTGTCCAAGTTTC	CGGTGCATGCATAGCCTTGT
$\beta$ -actin	ATCGTGCGGGACATCAAGG	TCGTTGCCGATGGTGATGAC

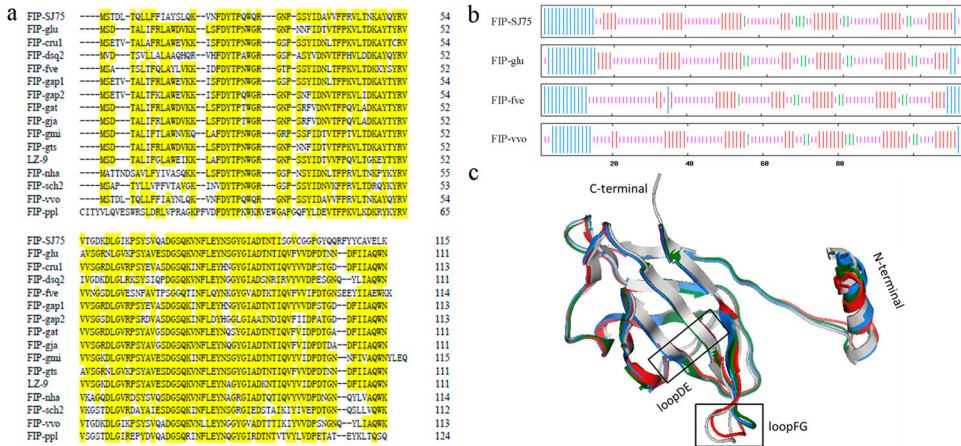


**Figure 1.** The sequence alignment, secondary structure prediction and structure model. (a) The sequence alignment was generated by Lasergene 7.1 software. The consensus residues were shaded as solid bright yellow. (b) Secondary structures of FIP-SJ75, FIP-glu, FIP-fve, and FIP-vvo predicted by SOPMA software online. The  $\alpha$ -helices,  $\beta$ -strands, and  $\beta$ -turns are indicated by blue, red, and green bars as shown. (c) The structures were modeled by MODOLLER 9.18 software. The main chain backbone of FIP-SJ75 (red) was superimposed perfectly with those of FIP-glu (blue), FIP-fve (sliver), and FIP-vvo (green). LoopDE and loopFG were highlighted in black rectangles.

And another lineage included FIP-dsq2, FIP-SJ75, and FIP-vvo. FIP-nha and FIP-ppl form a separate lineage, respectively (Figure 2(b)).

### 3.2. Production of rFIP-SJ75

To construct the expression plasmid, about 345-bp DNA fragment containing *FIP-SJ75* was cloned by PCR (Figure S1). After digested with *SacI* and *XbaI*, the fragment was inserted into pCold TF predigested with the same restriction enzymes (Figure S1). Besides, the pCold TF plasmid contains a  $6 \times$  His-tag to facilitate purification. The recombinant plasmid was designated as pCold TF-His-FIP-SJ75, as showing in Figure S1. According to the results of SDS-PAGE analysis, a distinct protein band was observed in the total cellular protein expressed in *E. coli* Rosetta (DE3) with pCold TF-His-FIP-SJ75, and the molecular mass of 65.6 kDa (Figure 3). Purification of the fusion protein was performed by one step using a TALON<sup>®</sup> metal affinity resin. The results of SDS-PAGE and Western blot analysis showed that the optimal induction time for rFIP-SJ75 was 24 h (Figure 4(a)). Besides, the rFIP-SJ75 could also be immunologically recognized by anti- $6 \times$  His antibody (Figure 4(b)). Subsequently, the His-tag and Trigger Factor were removed by Thrombin protease (Figure 4(c)). The purity of purified rFIPs was over 95% analyzed by SDS-PAGE. The yield of rFIP-SJ75 was 17.69 mg/L (after removing the His-tag and Trigger Factor), which was much higher than parental rFIPs (rFIP-glu, rFIP-fve, and rFIP-vvo). Furthermore, the results of LC/Q-TOF-MS showed that six peptides (Table 2) matched the amino acid sequences derived from rFIP-SJ75. The total sequence match reached 84.3%. Finally, we measured the LPS concentration in the purified rFIPs and determined that the LPS concentration was lower than 2.31 pg/ $\mu$ g



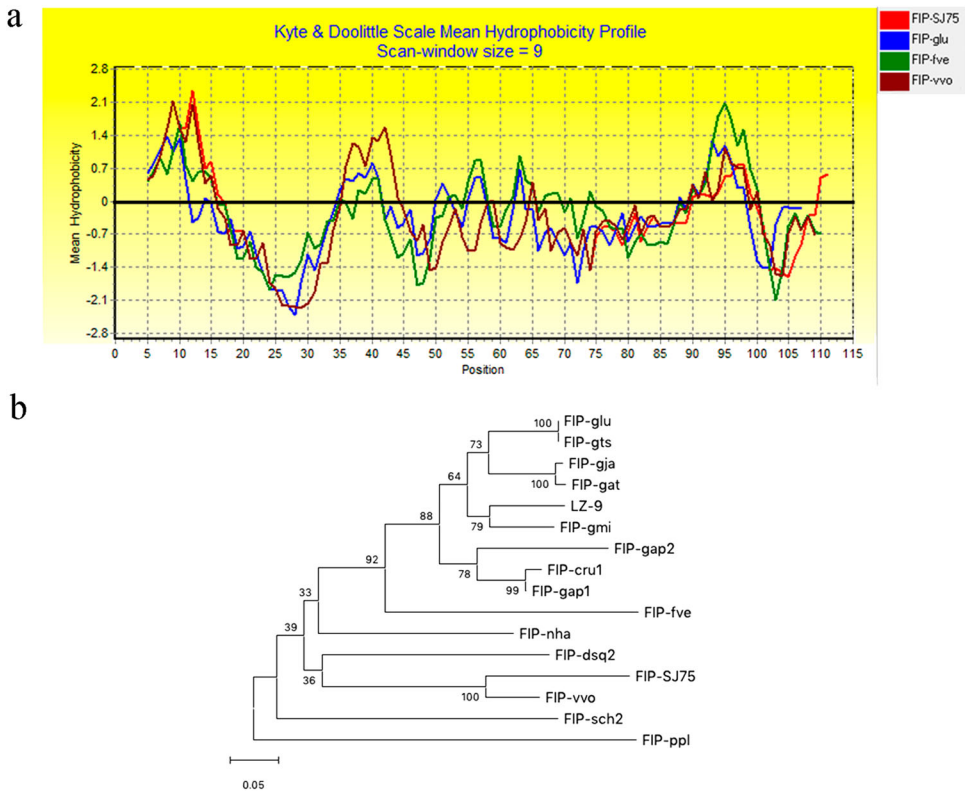


**Figure 2.** Hydrophobicity profile and phylogenetic tree construction. (a) The Kyte-Doolittle hydropathy index of FIP-SJ75 and other three parental proteins was analyzed by BioEdit 7.2.5 software. (b) The phylogenetic tree was constructed by MEGA7 software using the Neighbor-Joining method. Tree was generated based on the amino acid sequences of FIP-SJ75 and 15 reported FIPs.

protein. Due to the low content, it can be determined that LPS in rFIPs has little effect on cells in subsequent experiments and can be ignored.

### 3.3. Bioassay of rFIP-SJ75

#### 3.3.1. Toxicity of rFIP-SJ75 on RAW264.7 cells

To investigate the effect of rFIPs on the RAW264.7 cells, we must find out whether the four rFIPs possessed toxicity and determine the range of non-cytotoxic. The proliferation of RAW264.7 cells increased significantly ( $p < 0.0001$ ) when treated with 1 and 2  $\mu\text{g}/\text{mL}$  of rFIP-SJ75 compare to the control group. And when cells were exposed to 4 and 8  $\mu\text{g}/\text{mL}$  of rFIP-SJ75, the proliferation of RAW264.7 still increased ( $p < 0.01$ ). However, the proliferation rate of RAW264.7 cells resulted in no effect when incubated at the concentration of 16 and 32  $\mu\text{g}/\text{mL}$  of rFIP-SJ75 (Figure 5(a)). Besides, the proliferation of RAW264.7 cells revealed no significant difference when treated with 1, 16, and 32  $\mu\text{g}/\text{mL}$  of rFIP-glu compare to the control group. And rFIP-fve exhibited proliferation when 2, 4, and 8  $\mu\text{g}/\text{mL}$  of rFIP-glu treated RAW264.7 cells ( $p < 0.05$ ) (Figure 5(b)). When treated with 1 and 2  $\mu\text{g}/\text{mL}$  of rFIP-fve, the proliferation of RAW264.7 cells increased significantly ( $p < 0.0001$ ) relative to the control group. And when cells were exposed to 4, 8, and

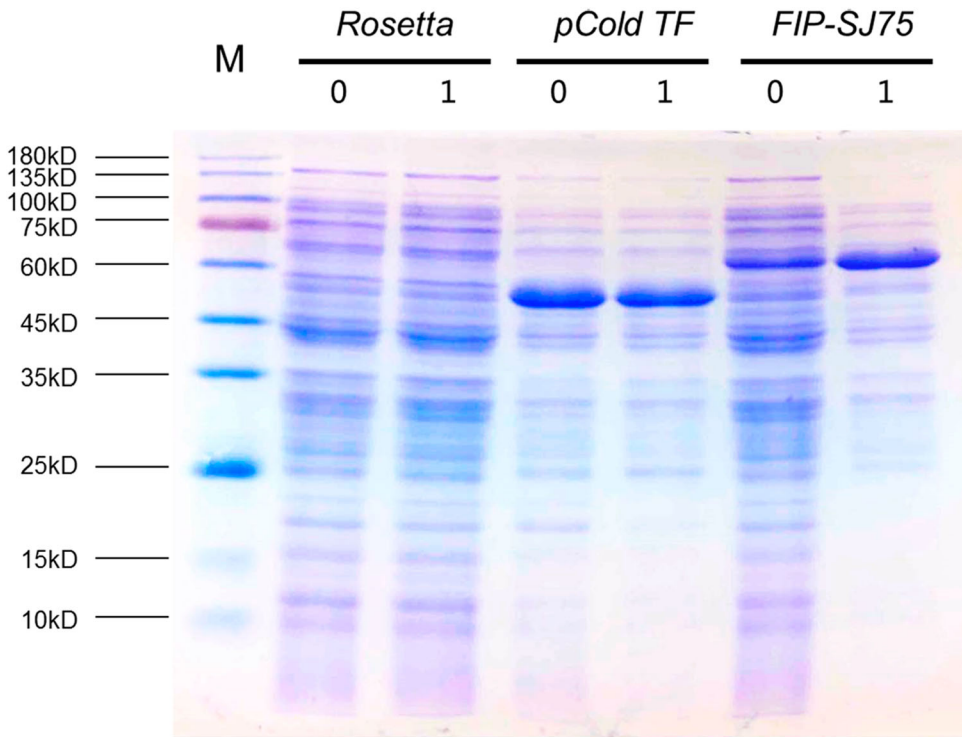


**Figure 3.** Analysis of the expression of rFIP-SJ75 by SDS-PAGE. Lane M: protein molecular mass marker; lane Rosetta: *E. coli* Rosetta (DE3) cells; lane pCold TF: *E. coli* Rosetta (DE3) cells containing expression vector pCold TF; lane FIP-SJ75: *E. coli* Rosetta (DE3) cells containing expression vector pCold TF-His-FIP-SJ75; lane 0: cells without IPTG treatment; lane 1: cells induced with IPTG.

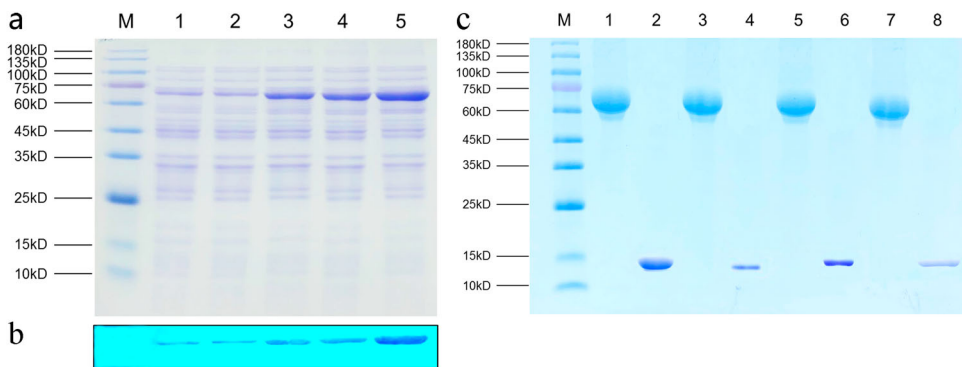


**Figure 4.** SDS-PAGE and Western blot of expression of FIP-SJ75 at different inducing times, SDS-PAGE of purified rFIPs. (a) Accumulation of rFIP-SJ75 protein in *E. coli* Rosetta (DE3) cells. Lane M: protein molecular mass marker; Lane 1–5: total cellular proteins collected 0, 4, 8, 12, and 24 h after IPTG induction, respectively. (b) Western blot detection of rFIP-SJ75 bands. Lane 1–5: samples collected 0, 4, 8, 12, and 24 h after IPTG induction, respectively. (c) Purified rFIPs analyzed by SDS-PAGE. Lane M: protein molecular mass marker; Lane 1, 3, 5, 7: purified rFIP-SJ75, rFIP-glu, rFIP-fve, and rFIP-vvo without removing His-tag and Trigger Factor; Lane 2, 4, 6, 8: purified rFIP-SJ75, rFIP-glu, rFIP-fve and rFIP-vvo removing His-tag and Trigger Factor.

**Table 2.** Peptide fragments identified from the tryptic digests of rFIP-SJ75.

Parent icon (m/z)	Peptide sequence
1619.7593	K.VNFLENSGYGIADTNTISGVCGGPGYQQR.F
798.0901	R.VVTGDKDLGIKPSYSVQADGSQK.V
761.3926	R.GNPSSYIDAVVFPR.V
596.7904	R.FYCAVELK
727.3538	K.VNFDYTPQWQR.G
628.3455	R.VLTNKAYQYR.V

16  $\mu\text{g}/\text{mL}$  of rFIP-fve, the proliferation of RAW264.7 showed no effect. While 32  $\mu\text{g}/\text{mL}$  of rFIP-fve treated RAW264.7 cells for 6 h, it exhibited toxicity ( $p < 0.05$ ) and the inhibitory was more than 10% (Figure 5(c)). A serially diluted concentration of rFIP-vvo showed no

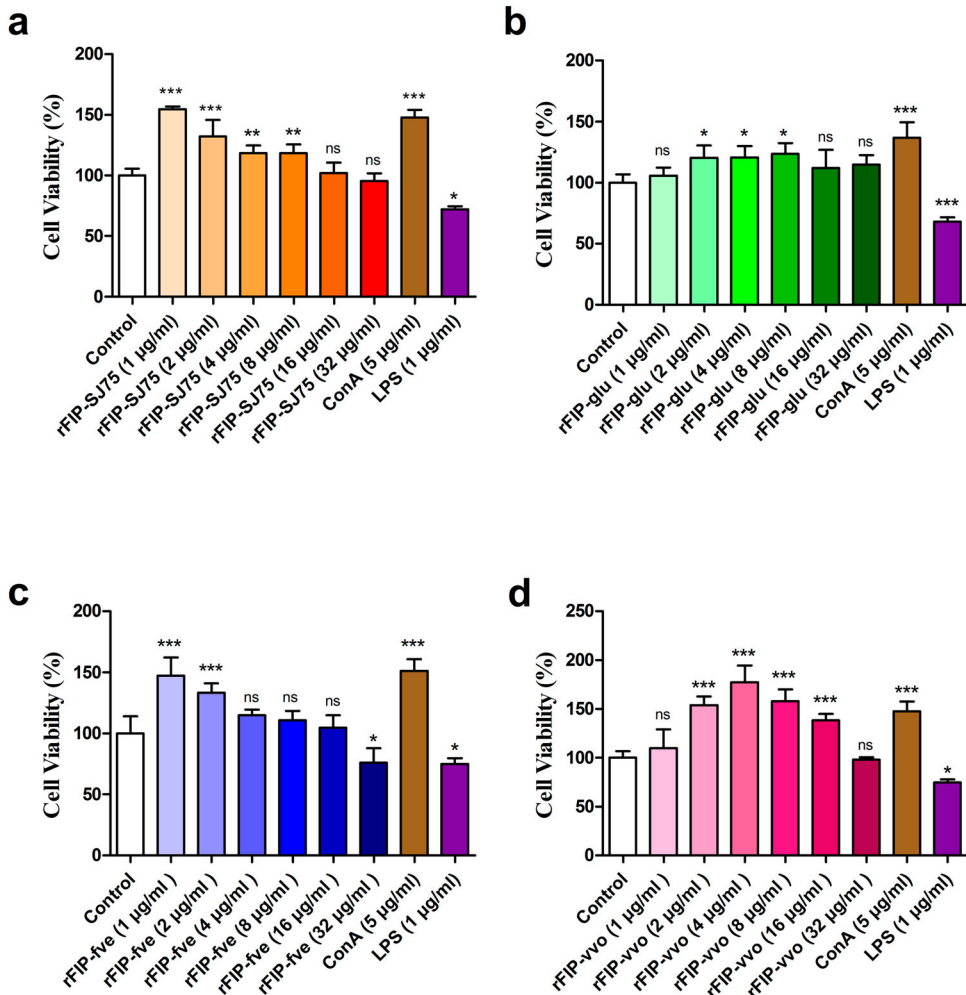


**Figure 5.** Effects of rFIPs on the viability of macrophage RAW264.7 cells. RAW264.7 cells were treated with different concentration of rFIPs (1, 2, 4, 8, 16, and 32  $\mu\text{g}/\text{mL}$ ), PBS as a control, ConA (5  $\mu\text{g}/\text{mL}$ ), and LPS (1  $\mu\text{g}/\text{mL}$ ) for 24 h. The cell viability was measured by CCK method. (a) RAW264.7 cell viability treated by rFIP-SJ75. (b) RAW264.7 cells viability treated by rFIP-glu. (c) RAW264.7 cells viability treated by rFIP-fve. (d) RAW264.7 cells viability treated by rFIP-vvo. Data were expressed as the mean  $\pm$  SD ( $n = 5$ ). *Ns*,  $p > 0.05$ ; \*,  $p < 0.05$ ; \*\*,  $p < 0.01$ ; \*\*\*,  $p < 0.0001$  versus control group.

toxicity to RAW264.7 cells. And when cells were exposed to 2, 4, 8, and 16  $\mu\text{g}/\text{mL}$  of rFIP-vvo, the proliferation of RAW264.7 increased significantly ( $p < 0.0001$ ) (Figure 5(d)). The above results suggested that the subsequent assays were performed with the concentration of rFIPs no more than 16  $\mu\text{g}/\text{mL}$ .

### 3.3.2. Phagocytosis of rFIP-SJ75 on RAW264.7 cells

The neutral red uptake assay was used to investigate the phagocytosis of rFIP-SJ75 on RAW264.7 cells. Then, RAW264.7 cells were treated with serially diluted non-cytotoxic concentrations of rFIP-SJ75 (1–16  $\mu\text{g}/\text{mL}$ ). The results showed that rFIP-SJ75 enhanced phagocytosis of RAW264.7 cells in a dose-dependent manner (Figure 6(a)). In order to compare the effect of different rFIPs on the phagocytosis, RAW264.7 cells were treated with purified rFIPs in a final concentration of 8  $\mu\text{g}/\text{mL}$ . The results suggested that the phagocytosis of rFIP-SJ75 on RAW264.7 cells was considerably higher than that of rFIP-glu ( $p < 0.01$ ), rFIP-fve ( $p < 0.05$ ) but no significant with rFIP-vvo (Figure 6(b)).

### 3.3.3. Inflammatory genes regulation of rFIP-SJ75 on RAW264.7 cells

To further determine the immunomodulatory effect of rFIP-SJ75 on macrophage RAW264.7 cells, 4 pro-inflammatory and anti-inflammatory related genes (*TNF- $\alpha$* , *IL-6*, *IL-10*, and *TGF- $\beta$ 1*) were chosen. The differential expression at the transcriptional level was examined by RT-qPCR. 8  $\mu\text{g}/\text{mL}$  of rFIP-SJ75-treated group showed a drastic increase in the mRNA level of *TNF- $\alpha$*  compared to the control ( $p < 0.0001$ ). Meanwhile, the results revealed that the mRNA level of *TNF- $\alpha$*  in the rFIP-SJ75-treated group was considerably lower than that of rFIP-fve ( $p < 0.0001$ ), but no significant difference with rFIP-glu and rFIP-vvo (Figure 7(a)). And rFIP-SJ75 also dramatically promoted the mRNA level of *IL-6* compared to the control ( $p < 0.0001$ ). In addition, the results showed that the mRNA level of *IL-6* promoting by rFIP-SJ75 was much higher than rFIP-glu ( $p <$

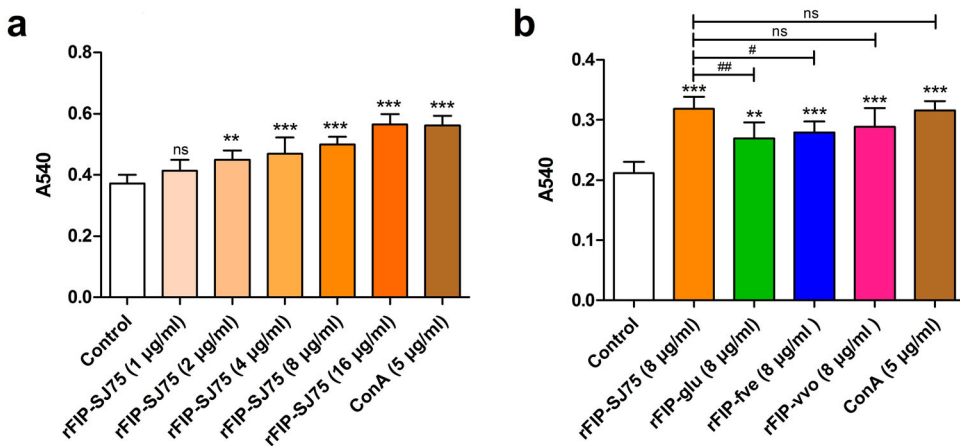


**Figure 6.** Effects of rFIPs on the phagocytosis of macrophage RAW264.7 cells. (a) RAW264.7 cells were treated with different concentration of rFIP-SJ75 (1, 2, 4, 8, and 16  $\mu\text{g}/\text{mL}$ ). PBS as a control and ConA (5  $\mu\text{g}/\text{mL}$ ) as a positive control. (b) RAW264.7 cells were treated with different rFIPs (8  $\mu\text{g}/\text{mL}$ ). The effects were assessed by neutral red uptake assay. Data were expressed as the mean  $\pm$  SD ( $n = 5$ ). Ns,  $p > 0.05$ ; \* or #,  $p < 0.05$ ; \*\* or ##,  $p < 0.01$ ; \*\*\* or ###,  $p < 0.0001$ .

0.0001) and rFIP-vvo ( $p < 0.0001$ ), but lower than rFIP-fve ( $p < 0.0001$ ) (Figure 7(b)). However, compared with control, the mRNA level of IL-10 treated with 8  $\mu\text{g}/\text{mL}$  of rFIP-SJ75 decreased ( $p < 0.0001$ ) (Figure 7(c)). Besides, rFIP-SJ75 inhibited the mRNA expression level of TGF- $\beta 1$  ( $p < 0.0001$ ). The results showed that the mRNA level of TGF- $\beta 1$  in the rFIP-SJ75-treated group was significantly lower than that of rFIP-vvo ( $p < 0.0001$ ), but no change compared with rFIP-glu and rFIP-fve (Figure 7(d)). These results demonstrated that rFIP-SJ75 had the effect of immunomodulatory on macrophage, which could obviously promote pro-inflammatory genes (*TNF- $\alpha$*  and *IL-6*), but reduce the anti-inflammatory genes (*IL-10* and *TGF- $\beta 1$* ) expression at the transcriptional level.

#### 4. Discussion

This is the first study to reveal that FIP-SJ75, a novel immunomodulatory protein generated from three genus of mushrooms (*G. lucidum*, *F. velutipes*, and *V. volvacea*) by DNA

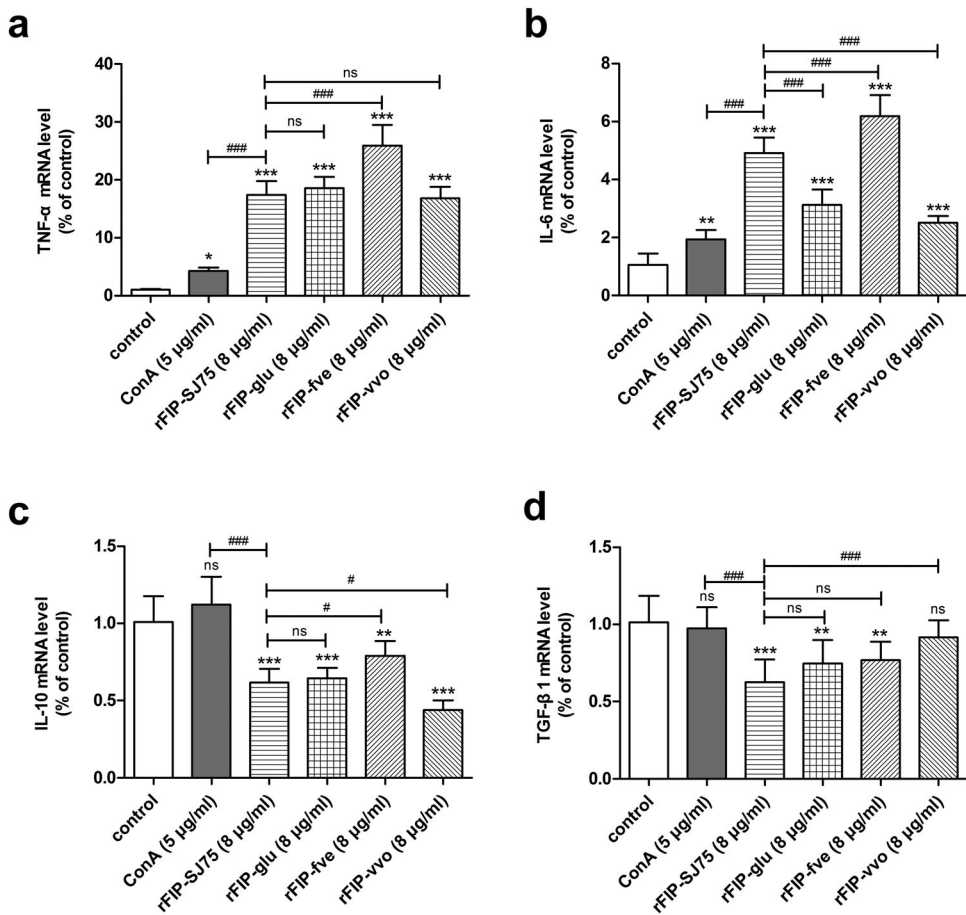


**Figure 7.** Effects of rFIPs on macrophage RAW264.7 cells. The cells were treated with rFIPs (8  $\mu\text{g}/\text{mL}$ ) for 6 h. PBS as a control and ConA (5  $\mu\text{g}/\text{mL}$ ) as a positive control. The mRNA expression of TNF- $\alpha$  (a), IL-6 (b), IL-10 (c), TGF- $\beta 1$  (d) was measured by qRT-PCR. Data were expressed as the mean  $\pm$  SD ( $n = 3$ ). Ns,  $p > 0.05$ ; \* or #,  $p < 0.05$ ; \*\* or ##,  $p < 0.01$ ; \*\*\* or ###,  $p < 0.0001$ .

shuffling, is a potent activator of mouse macrophages. Since the first fungal immunomodulatory protein, FIP-glu (LZ-8), was isolated from the fruiting body of *G. lucidum*, FIPs have attracted the attention of research in the fields of biochemistry and pharmacology (Li et al., 2011). However, extracting FIPs from natural mushrooms remains time-consuming, low yield, and costly. Thus researchers have attempted to obtain more biologically active recombinant FIPs from various host cells (Kong et al., 2013). It is well known that prokaryotic expression is an important method to express exogenous genes. In addition, previous research proved that the quantity of expression is always affected by the choice of the vector. Unfortunately, our previous studies showed that rFIP-SJ75 expressed with the pET vector is an insoluble inclusion body protein with low yields that are not conducive to mass production. In this study, we chose pCold TF expression vector to gain soluble rFIPs, and the yield of FIP-SJ75 reached 17.69 mg/L in *E.coli* strain Rosetta (DE3) cells. The pCold TF is a DNA vector triggered by cold shock to optimize the co-translational folding process of nascent polypeptides and contains a His-tag tag commonly used to express proteins that readily form inclusion bodies. The amino acid sequence alignment showed FIP-SJ75 shared 49.1%–94.7% homology with other FIPs (Figure 1(a)). The Sopma secondary structure prediction showed that FIP-SJ75 possessed two  $\alpha$ -helixed and seven extended-strands, similar to other FIPs (Figure 1(b)). The predicted structure of FIP-SJ75 can be superimposed on those of the other three parental proteins, except in the N-terminal, loopDE, and loopFG regions (Figure 1(c)). These structural differences were thought to be the reason why the FIPs of *Ganoderma spp* strongly exhibited direct anti-tumor activities, but FIP-fve weakly (Huang et al., 2009). Furthermore, the N-terminal  $\alpha$ -helix region was believed to be significant to recognize surface receptors and form dimers (Lin, Hung, Hsu, & Lin, 1997). Structural differences indicated that certain biological activities of FIP-SJ75 might be more similar to FIP-fve than FIP-glu and FIP-vvo. The hydrophobicity profile showed that FIP-SJ75 had similar hydrophobicity and hydrophilicity to the other three parental proteins (Figure 2(a)). However, some differences were still observed among certain regions of different FIPs, which might influence the structure and biological activity. Furthermore, the phylogenetic tree indicated that FIP-SJ75 had a substantial difference with other FIPs, except for FIP-vvo. (Figure 2(b)) Therefore, we supposed that FIP-SJ75 was a new member of the FIP family. Thus, FIP-SJ75 and other three FIPs (FIP-glu, FIP-fve, and FIP-vvo) were synthesized, cloned, expressed, and examined for their biological activities *in vitro*.

It is well recognized that many chronic diseases, such as cancer are associated with inflammation tightly. Besides, inflammation is also a precursor to the onset of many chronic diseases (Yuan et al., 2017). Macrophages are an important part of the immune system, which also plays key roles in host defense against bacterial infections and inhibiting the growth of tumour cells. Macrophages initiate innate immune responses by swallowing exogenous pathogens (Aderem & Underhill, 1999). It has been reported that polysaccharides (ADPs-1a and ADPs-3a) and FIPs (LZ-8) have a strong promoting effect on phagocytosis of RAW264.7 cells (Li, Chang et al., 2019; Wang et al., 2019). Similar to the conclusions of the above studies, the neutral red assay showed that rFIP-SJ75 at the concentration of 4–16  $\mu\text{g}/\text{mL}$  significantly promoted the phagocytosis of RAW264.7 cells ( $p < 0.0001$ ). Besides, rFIP-SJ75 had a stronger effect on improving the phagocytic ability of macrophages compared with rFIP-glu and rFIP-fve at 8  $\mu\text{g}/\text{mL}$ . However, there was no significant difference between rFIP-SJ75 and rFIP-vvo in

enhancing the phagocytosis of RAW264.7 cells. We supposed that it might be attributed to the similar affinities and structures of FIP-SJ75 and FIP-vvo.

Macrophages play a role in the immune system by phagocytizing exogenous pathogens and releasing cytokine inflammatory mediators (Arango Duque and Descoteaux 2014). Depending on the identity of the activating signals, macrophages can be divided into two types: classically activated macrophages (M1) and alternatively activated macrophages (M2), respectively (Vergadi, Ieronymaki, Lyroni, Vaporidi, & Tsatsanis, 2017; Wang et al. 2014). M1 macrophages secrete pro-inflammatory cytokines (TNF- $\alpha$ , IL-1 $\beta$ , IL-6, etc.), chemokines (CCL-2, CXCL-10, etc.), and nitric oxide (NO), whereas M2 macrophages secrete high level of anti-inflammatory cytokines (IL-8, IL-10, TGF- $\beta$ 1, etc.) (Qin et al., 2012; Shapouri-Moghaddam et al., 2018). The level of inflammation-associated cytokines in macrophages can be used as an indicator to assess the ability of biologically active substances to stimulate immune response (Cheong et al., 2016). In this study, rFIP-SJ75 and other three rFIPs (FIP-glu, FIP-fve, and FIP-vvo) could stimulate the mRNA expression level of TNF- $\alpha$  and IL-6 in RAW264.7 cells significantly. Among the four purified rFIPs, rFIP-fve showed the strongest effect on enhancing the mRNA expression level of pro-inflammatory cytokines at the same concentration. Moreover, the mRNA level of IL-10 was inhibited by rFIP-SJ75, rFIP-glu, rFIP-fve, and rFIP-vvo. At the same time, rFIP-SJ75, rFIP-glu, and rFIP-fve inhibited the mRNA level of TGF- $\beta$ 1. It is well recognized that TNF- $\alpha$  is a pro-inflammatory cytokine and plays an essential role in the immune responses and inflammation (Ng et al., 2018). IL-6 is an interleukin that can be secreted by macrophages and promotes the proliferation and differentiation of B cells and T cells (Davies et al., 2013). However, IL-10 and TGF- $\beta$ 1 have an inhibitory effect on inflammatory responses and belong to Treg cytokines (Chu et al., 2017). In this study, there was an increase in the level of TNF- $\alpha$  and IL-6, while a decrease or little change in the level of IL-10 and TGF- $\beta$ 1, which suggested that rFIP-SJ75 exerted immunomodulatory by promoting macrophage M1 polarization and initiating pro-inflammatory responses.

Toll-like receptor (TLR) family can activate macrophages (Hug et al., 2018). Activated TLRs induce the signalling pathways within specific cells, such as MAPKs and NF- $\kappa$ B. MAPKs and NF- $\kappa$ B are classical inflammation-related signals, which can induce the expression of the pro-inflammatory mediators (Li, Chang et al., 2019; Vergadi et al., 2017). In this study, we have proved that rFIP-SJ75 and other three parental rFIPs could activate macrophages and enhance the mRNA expression level of pro-inflammatory cytokines. Thus, we suppose that rFIP-SJ75 can enter cells directly or be bind to TLR4 indirectly to activate downstream signalling pathways such as MAPKs/NF- $\kappa$ B. Then, it will stimulate the phosphorylation of p38, ERK, JNK, and NF- $\kappa$ B, thereby transferring from cytoplasm to nucleus and promoting the production of pro-inflammatory cytokines (Figure 8).

In conclusion, a novel FIP shuffled from different mushroom species, designated as FIP-SJ75, was confirmed and presented a certain degree of similarity with the reported FIPs in sequence identity, structure, hydrophobicity, and evolutionary conservation. *In vitro* bioactivity assay showed that rFIP-SJ75 had a stronger effect on promoting the phagocytosis of RAW264.7 cells, but the same effect on being an activator of M1 macrophage polarization compared with other three parental rFIPs. Besides, rFIP-SJ75 could enhance the mRNA expression of TNF- $\alpha$  and IL-6 on the RAW264.7 cells. However, further work is required to figure out how rFIP-SJ75 regulates the inflammatory cytokines.

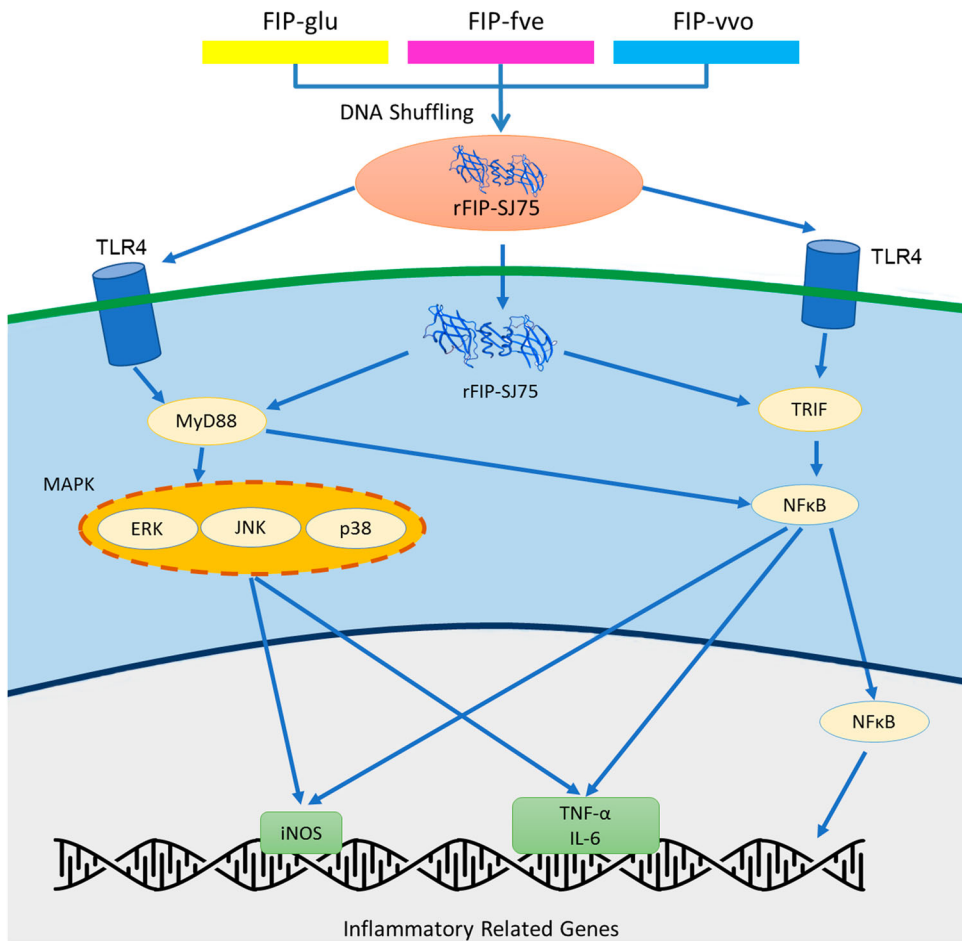


**Figure 8.** Possible immunomodulatory signalling mechanism of rFIP-SJ75 in RAW264.7 macrophages. FIP, fungal immunomodulatory protein; TLR, Toll-like receptor; MyD88, myeloid differentiation factor 88; TRIF, Toll-interleukin 1 receptor domain-containing adapter inducing interferon- $\beta$ ; MAPK, mitogen activated protein kinase; NF- $\kappa$ B, nuclear factor kappa B; ERK, extracellular signal regulated kinase; JNK, c-Jun NH2-terminal kinase; TNF- $\alpha$ , tumour necrosis factor-alpha; IL-6, interleukin-6; iNOS, inducible nitric oxide synthase.

Nevertheless, our study indicates that rFIP-SJ75 has potential as immunomodulatory agents for certain inflammation-related diseases.

## Acknowledgments

We would like to thank Ying Wang from Shanghai Academy of Agricultural Sciences helping us to build a homology model of the 3D structure of FIP-SJ75 using the crystal structures of FIP-glu and FIP-fve as templates. We also thank the technicians in instrumental analysis center of SJTU for their helping to perform LC/Q-TOF-MS analysis of rFIP-SJ75.

## Disclosure statement

No potential conflict of interest was reported by the authors.



## Funding

This research was financially supported by the Fujian Puzhiyun Biological Technology Co., Ltd, under [grant number 19H100000393], the Natural Science Foundation of Shanghai under [grant number 18ZR1420600], and the Shanghai Science and Technology Innovation Action Plan under [grant number 19431901700].

## Ethical statement

This article does not contain any studies with human participants or animals performed by any of the authors.

## ORCID

Xuan-Wei Zhou  <http://orcid.org/0000-0002-3993-6346>

## References

- Aderem, A., & Underhill, D. M. (1999). Mechanisms of phagocytosis in macrophages. *Annual Review of Immunology*, 17(1), 593–623. doi:10.1146/annurev.immunol.17.1.593
- Arango Duque, G., & Descoteaux, A. (2014). Macrophage cytokines: Involvement in immunity and infectious diseases. *Frontiers in Immunology*, 5, 491. doi:10.3389/fimmu.2014.00491
- Bastiaan-Net, S., Chanput, W., Hertz, A., Zwitterink, R. D., Mes, J. J., & Wichers, H. J. (2013). Biochemical and functional characterization of recombinant fungal immunomodulatory proteins (rFIPs). *International Immunopharmacology*, 15(1), 167–175. doi:10.1016/j.intimp.2012.11.003
- Chang, H. H., Yeh, C. H., & Sheu, F. (2009). A novel immunomodulatory protein from *Poria cocos* induces Toll-like receptor 4-dependent activation within mouse peritoneal macrophages. *Journal of Agricultural and Food Chemistry*, 57(14), 6129–6139. doi:10.1021/jf9011399
- Cheong, K. L., Meng, L. Z., Chen, X. Q., Wang, L. Y., Wu, D. T., Zhao, J., & Li, S.-P. (2016). Structural elucidation, chain conformation and immuno-modulatory activity of glucogalactomannan from cultured *Cordyceps sinensis* fungus UM01. *Journal of Functional Foods*, 25, 174–185. doi:10.1016/j.jff.2016.06.002
- Chu, P. Y., Sun, H. L., Ko, J. L., Ku, M. S., Lin, L. J., Lee, Y. T., ... Lue, K. H. (2017). Oral fungal immunomodulatory protein-*Flammulina velutipes* has influence on pulmonary inflammatory process and potential treatment for allergic airway disease: A mouse model. *Journal of Microbiology, Immunology and Infection*, 50(3), 297–306. doi:10.1016/j.jmii.2015.07.013
- Cong, W. R., Xu, H., Liu, Y., Li, Q. Z., Li, W., & Zhou, X. W. (2014). Production and functional characterization of a novel fungal immunomodulatory protein FIP-SN15 shuffled from two genes of *Ganoderma* species. *Applied Microbiology and Biotechnology*, 98(13), 5967–5975. doi:10.1007/s00253-014-5539-4
- Davies, L. C., Jenkins, S. J., Allen, J. E., & Taylor, P. R. (2013). Tissue-resident macrophages. *Nature Immunology*, 14(10), 986–995. doi:10.1038/ni.2705
- Felsenstein, J. (1985). Confidence limits on phylogenies: An approach using the bootstrap. *Evolution*, 39(4), 783–791. doi:10.1111/j.1558-5646
- Gao, Y., Wang, Y., Wang, Y., Wu, Y. Y., Chen, H. Y., Yang, R. H., & Bao, D. P. (2019). Protective function of novel fungal immunomodulatory proteins Fip-lti1 and Fip-lti2 from *Lentinus tigrinus* in concanavalin a-induced liver oxidative injury. *Oxidative Medicine and Cellular Longevity*. doi:10.1155/2019/3139689
- Hsu, H. C., Hsu CI, L. I. N. R. H., Kao, C. L., & Lin, J. W. (1997). Fip-vvo, a new fungal immunomodulatory protein isolated from *Volvariella volvacea*. *Biochemical Journal*, 323(2), 557–565. doi:10.1042/bj3230557

- Huang, L., Sun, F., Liang, C., He, Y. X., Bao, R., Liu, L., & Zhou, C. Z. (2009). Crystal structure of LZ-8 from the medicinal fungus *Ganoderma lucidum*. *Proteins: Structure, Function, and Bioinformatics*, 75(2), 524–527. doi:10.1002/prot.22346
- Hug, H., Mohajeri, M., & La Fata, G. (2018). Toll-like receptors: Regulators of the immune response in the human gut. *Nutrients*, 10(2), 203. doi:10.3390/nu10020203
- Kino, K., Yamashita, A., Yamaoka, K., Watanabe, J., Tanaka, S., Ko, K., ... Tsunoo, H. (1989). Isolation and characterization of a new immunomodulatory protein, ling zhi-8 (LZ-8), from *Ganoderma lucidum*. *Journal of Biological Chemistry*, 264(1), 472–478. doi:10.1021/bi00427a056
- Ko, J. L., Hsu, C. I., Lin, R. H., Kao, C. L., & Lin, J. Y. (1995). A new fungal immunomodulatory protein, FIP-fve isolated from the edible mushroom, *Flammulina velutipes* and its complete amino acid sequence. *European Journal of Biochemistry*, 228(2), 244–249. doi:10.1111/j.1432-1033.1995.0244n.x
- Kong, X. H., Zhang, J., Han, X., Zhang, P. Q., Dai, X. D., Liu, J. N., ... Liu, S. K. (2013). High-yield production in *Escherichia coli* of fungal immunomodulatory protein isolated from *Flammulina velutipes* and its bioactivity assay *in vivo*. *International Journal of Molecular Sciences*, 14(2), 2230–2241. doi:10.3390/ijms14022230
- Lee, S. J., & Lim, K. T. (2008). Phytoglycoprotein inhibits interleukin-1 $\beta$  and interleukin-6 via p38 mitogen-activated protein kinase in lipopolysaccharide-stimulated RAW 264.7 cells. *Naunyn-Schmiedeberg's Archives of Pharmacology*, 377(1), 45–54. doi:10.1007/s00210-007-0253-8
- Leiro, J. M., Castro, R., Arranz, J. A., & Lamas, J. (2007). Immunomodulating activities of acidic sulphated polysaccharides obtained from the seaweed *Ulva rigida* C. Agardh. *International Immunopharmacology*, 7(7), 879–888. doi:10.1016/j.intimp.2007.02.007
- Li, F., Wen, H. A., Liu, X. Z., Zhou, F. Z., & Chen, G. C. (2012). Gene cloning and recombinant expression of a novel fungal immunomodulatory protein from *Trametes versicolor*. *Protein Expression and Purification*, 82(2), 339–344. doi:10.1016/j.pep.2012.01.015
- Li, H. B., Bu, X. F., Li, K., & Wu, D. H. (2019). Production of a novel *Poria cocos* immunomodulatory protein in *Pichia pastoris*: Cloning, expression, purification and activities assays. *World Journal of Microbiology and Biotechnology*, 35(2), 27. doi:10.1007/s11274-019-2602-4
- Li, Q. Z., Wang, X. F., & Zhou, X. W. (2011). Recent status and prospects of the fungal immunomodulatory protein family. *Critical Reviews in Biotechnology*, 31(4), 365–375. doi:10.3109/07388551.2010.543967
- Li, Q. Z., Chang, Y. Z., He, Z. M., Chen, L., & Zhou, X. W. (2019). Immunomodulatory activity of *Ganoderma lucidum* immunomodulatory protein via PI3K/Akt and MAPK signaling pathways in RAW264.7 cells. *Journal of Cellular Physiology*. doi:10.1002/jcp.28901
- Li, S. Y., Jiang, Z. H., Sun, L. C., Liu, X., Huang, Y., Wang, F. Z., & Xin, F. J. (2017). Characterization of a new fungal immunomodulatory protein, FIP-dsq2 from *Dichomitus squalens*. *Journal of Biotechnology*, 246, 45–51. doi:10.1016/j.jbiotec.2017.02.006
- Li, S. Y., Shi, L. J., Ding, Y., Nie, Y., & Tang, X. M. (2015). Identification and functional characterization of a novel fungal immunomodulatory protein from *Postia placenta*. *Food and Chemical Toxicology*, 78, 64–70. doi:10.1016/j.fct.2015.01.013
- Lin, J. W., Guan, S. Y., Duan, Z. W., Shen, Y. H., Fan, W. L., Chen, L. J., ... Li, T. L. (2016). Gene cloning of a novel fungal immunomodulatory protein from *Chroogomphis rutilus* and its expression in *Pichia pastoris*. *Journal of Chemical Technology & Biotechnology*, 91(11), 2761–2768. doi:10.1002/jctb.4881
- Lin, W. H., Hung, C. H., Hsu, C. I., & Lin, J. Y. (1997). Dimerization of the N-terminal amphipathic  $\alpha$ -helix domain of the fungal immunomodulatory protein from *Ganoderma tsugae* (Fip-gts) defined by a yeast two-hybrid system and site-directed mutagenesis. *Journal of Biological Chemistry*, 272(32), 20044–20048. doi:10.1074/jbc.272.32.20044
- Ng, A., Tam, W. W., Zhang, M. W., Ho, C. S., Husain, S. F., McIntyre, R. S., & Ho, R. C. (2018). IL-1 $\beta$ , IL-6, TNF- $\alpha$  and CRP in elderly patients with depression or Alzheimer's disease: Systematic review and meta-analysis. *Scientific Reports*, 8(1), 12050. doi:10.1038/s41598-018-30487-6
- Nonnenmacher, Y., & Hiller, K. (2018). Biochemistry of proinflammatory macrophage activation. *Cellular and Molecular Life Sciences*, 75(12), 2093–2109. doi:10.1007/s00018-018-2784-1

- Qin, H., Holdbrooks, A. T., Liu, Y., Reynolds, S. L., Yanagisawa, L. L., & Benveniste, E. N. (2012). SOCS3 deficiency promotes M1 macrophage polarization and inflammation. *The Journal of Immunology*, 189(7), 3439–3448. doi:10.4049/jimmunol.1201168
- Shapouri-Moghaddam, A., Mohammadian, S., Vazini, H., Taghadosi, M., Esmaeili, S. A., Mardani, F., ... Sahebkar, A. (2018). Macrophage plasticity, polarization, and function in health and disease. *Journal of Cellular Physiology*, 233(9), 6425–6440. doi:10.1002/jcp.26429
- Sheu, F., Chien, P. J., Chien, A. L., Chen, Y. F., & Chin, K. L. (2004). Isolation and characterization of an immunomodulatory protein (APP) from the Jew's Ear mushroom *Auricularia polytricha*. *Food Chemistry*, 87(4), 593–600. doi:10.1016/j.foodchem.2004.01.015
- Sica, A., Erreni, M., Allavena, P., & Porta, C. (2015). Macrophage polarization in pathology. *Cellular and Molecular Life Sciences*, 72(21), 4111–4126. doi:10.1007/s00018-015-1995-y
- Vergadi, E., Ieronymaki, E., Lyroni, K., Vaporidi, K., & Tsatsanis, C. (2017). Akt signaling pathway in macrophage activation and M1/M2 polarization. *The Journal of Immunology*, 198(3), 1006–1014. doi:10.4049/jimmunol.1601515
- Wang, X. F., Li, Q. Z., Bao, T. W., Cong, W. R., Song, W. X., & Zhou, X. W. (2013). *In vitro* rapid evolution of fungal immunomodulatory proteins by DNA family shuffling. *Applied Microbiology and Biotechnology*, 97(6), 2455–2465. doi:10.1007/s00253-012-4131-z
- Wang, N., Liang, H., & Zen, K. (2014). Molecular mechanisms that influence the macrophage M1–M2 polarization balance. *Frontiers in Immunology*, 5, 614. doi:10.3389/fimmu.2014.00614
- Wang, X. F., Su, K. Q., Bao, T. W., Cong, W. R., Chen, Y. F., Li, Q. Z., & Zhou, X. W. (2012). Immunomodulatory effects of fungal proteins. *Current Topics in Nutraceuticals Research*, 10(1), 1. doi:10.5897/AJPP11.626
- Wang, J., Wang, H., Zhang, H., Liu, Z., Ma, C., & Kang, W. (2019). Immunomodulation of ADPs-1a and ADPs-3a on RAW264. 7 cells through NF-κB/MAPK signaling pathway. *International Journal of Biological Macromolecules*, 132, 1024–1030. doi:10.1016/j.ijbiomac.2019.04.031
- Williams, A. F., & Barclay, A. N. (1988). The immunoglobulin superfamily—domains for cell surface recognition. *Annual Review of Immunology*, 6(1), 381–405. doi:10.1146/annurev.iy.06.040188.002121
- Wu, M., Hsu, M., Huang, C. S., Fu, H., Huang, C. T., & Yang, C. S. (2007). A 2.0 Å structure of GMI, a member of the fungal immunomodulatory protein family from *Ganoderma microsporum*. *Protein Crystallogr*, 2, 132.
- Xiong, L., Ouyang, K. H., Jiang, Y., Yang, Z. W., Hu, W. B., Chen, H., ... Wang, W. J. (2018). Chemical composition of *Cyclocarya paliurus* polysaccharide and inflammatory effects in lipopolysaccharide-stimulated RAW264.7 macrophage. *International Journal of Biological Macromolecules*, 107, 1898–1907. doi:10.1016/j.ijbiomac.2017.10.055
- Xu, H., Kong, Y. Y., Chen, X., Guo, M. Y., Bai, X. H., Lu, Y. J., ... Zhou, X. W. (2016). Recombinant FIP-gat, a fungal immunomodulatory protein from *Ganoderma atrum*, induces growth inhibition and cell death in breast cancer cells. *Journal of Agricultural and Food Chemistry*, 64(13), 2690–2698. doi:10.1021/acs.jafc.6b00539
- Yuan, B., Zhao, L., Rakariyatham, K., Han, Y., Gao, Z., Kimatu, B. M., ... Xiao, H. (2017). Isolation of a novel bioactive protein from an edible mushroom *Pleurotus eryngii* and its anti-inflammatory potential. *Food & Function*, 8(6), 2175–2183. doi:10.1039/c7fo00244k
- Zhou, S. Y., Guan, S. X., Duan, Z. W., Han, X., Zhang, X., Fan, W. L., ... Lin, J. (2018). Molecular cloning, codon-optimized gene expression, and bioactivity assessment of two novel fungal immunomodulatory proteins from *Ganoderma applanatum* in *Pichia*. *Applied Microbiology and Biotechnology*, 102(13), 5483–5494. doi:10.1007/s00253-018-9022-5
- Zhou, X. W., Xie, M., Hong, F., & Li, Q. Z. (2009). Genomic cloning and characterization of a FIP-gsi gene encoding a fungal immunomodulatory protein from *Ganoderma sinense* Zhao et al.(Aphyllphoromycetidae). *International Journal of Medicinal Mushrooms*, 11(1). doi:10.1615/IntJMedMushr.v11.i1.90